

PION PRODUCTION

DIFFERENTIAL CROSS SECTION AND ANALYZING POWER OF $p(\vec{p}, \pi^+)d$ NEAR THRESHOLD

P. Heimberg, R.E. Segel, and F. Chen
Northwestern University, Evanston, Illinois 60201

R.D. Bent, J. Blomgren, H.O. Meyer, H. Nann,
B. von Przewoski, T. Rinckel, and A. Zhuralev
Indiana University Cyclotron Facility, Bloomington, Indiana 47408

M. Pickar
University of Kentucky, Lexington, Kentucky 40506

G. Hardie and P. Pancella
Western Michigan University, Kalamazoo, Michigan 49008

E. Jacobsen
Princeton University, Princeton, New Jersey 07544

J.D. Brown
Yale University, New Haven, Connecticut 06511

The $NN \rightarrow d\pi$ and $NN \rightarrow NN\pi$ reactions in the threshold region give direct information about non-resonant pion production mechanisms. Using the IUCF Cooler, with its well-defined beam energy ($\Delta E \simeq 50$ keV), high luminosity ($10^{30}/\text{cm}^2\text{s}$), internal targets and low background, it is possible to make measurements very much closer to threshold than had previously been achieved. Experiment CE-31 was run in April of 1993. We measured analyzing powers and cross sections at nine energies corresponding to $\eta = p_{\pi}^{cm}/m_{\pi}c$ in the range 0.02 to 0.20. This constitutes the first simultaneous measurement of cross sections and analyzing powers for pion production in the region where p-wave contributions are expected to be negligibly small.

The measurement was carried out in the G-region of the Cooler ring using a 70% polarized proton beam and a hydrogen gas jet target. The detector was comprised of left-right symmetric plastic scintillator stacks which measured the dE/dx and E of the produced pions, protons and deuterons. Any particles that punched through the ΔE and E counters were vetoed by another set of plastic scintillators. Near threshold the deuterons coming from $pp \rightarrow d\pi^+$ have a maximum lab angle $\simeq 1^\circ$ and are therefore lost down the beam pipe and cannot be used to tag pions.

CE31 Detector Stack

(Top View , Schematic)

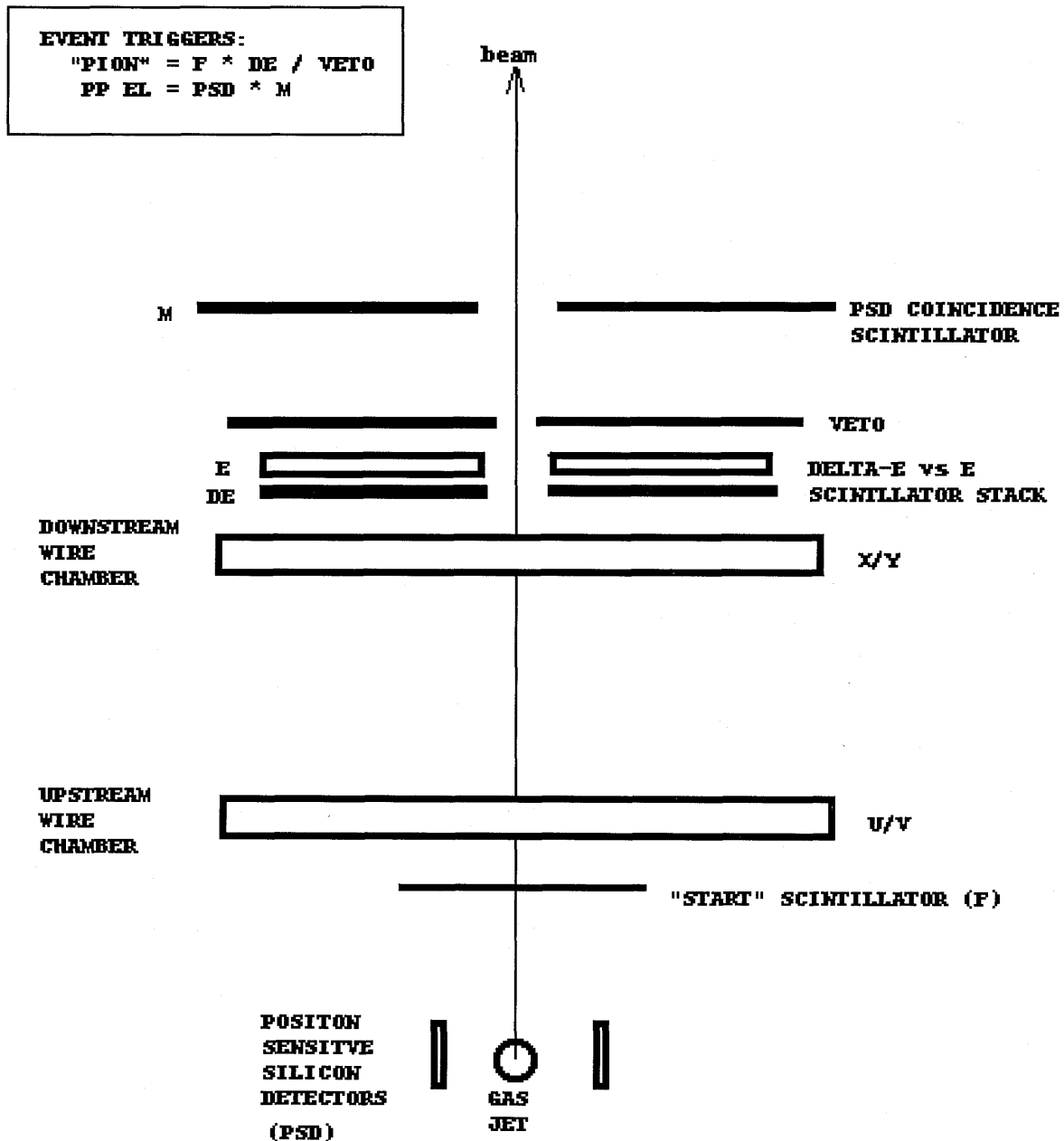


Figure 1. Schematic of detector layout. The distance between the F-detector and the $\Delta E-E$ stack is 80 cm.

The pp elastic scattering channel served as both the luminosity monitor and the polarimeter. Elastic proton events were defined by the coincidence between a forward-going proton ($5^\circ \leq \Theta_{lab} \leq 20^\circ$) in the plastic scintillator stack and large-angle proton in a position sensitive silicon detector (PSD). Lab angles for all emergent particles were measured by two double-planed wire chambers each of which gave vertical and horizontal positions. Figure 1 shows a schematic of the detector layout. The wire chambers, PSD's, and jet target were originally constructed for and used in CE-01 which measured the $pp \rightarrow pp\pi^0$ total cross section.

The pions are identified in several ways. The primary identification comes from a simple ΔE vs. E scheme. Figure 2 illustrates that protons stopped in the stack are cleanly separated from the stopped pions. Time-of-flight vs. E also gives clear separation. Figure 3 shows Time-of-flight vs. E for those pions, protons and deuterons that stopped in the ΔE counter. Besides energy loss and time-of-flight, a simple scheme for pion identification via $\pi^+ \rightarrow \mu^+ \nu$ is also employed. The analog signal coming from a stable particle is a simple prompt pulse coming from the kinetic energy deposited as it comes to rest. For pions, the signal has two components: (1) the prompt pulse from kinetic energy deposition and (2) a delayed pulse coming from the decay muon's deposited kinetic energy ($\simeq 4$ MeV). Such events are identified by splitting the signal and applying gates of different lengths to the ADC's. One gate is extremely short ($\simeq 10$ ns) and just barely contains the prompt pulse. The other gate is much longer ($\simeq 150$ ns) and contains both the prompt pulse and the delayed pulse. The difference between the two measured energies is zero for stable particles and 4 MeV for pions. The efficiency for tagging the pions in this way is only about 60%, but the background is completely eliminated. Figure 4 shows a typical difference spectrum for one of the pion-stopping scintillators. Figure 5 shows half of the kinematically characteristic "parabola" the pions form in a plot of Θ_{lab} vs. E . These data are for $\eta = 0.09$, which corresponds to a maximum lab angle of 13.2° .

From the measurement of σ_{tot} , $d\sigma/d\Omega$, and A_y sufficiently close to threshold and from Watson's theorem the s-wave amplitude can be determined accurately. The analyzing power, being sensitive to the interference between the s- and p-wave amplitudes, gives a good measure of the total p-wave contribution to the cross section.

While this measurement does give the total p-wave contribution, nothing can be said about the individual p-wave components corresponding to initial proton 1S_0 and 1D_2 states. Installation of a polarized hydrogen target which could be used for such measurements in the not-so-distant future is currently underway.

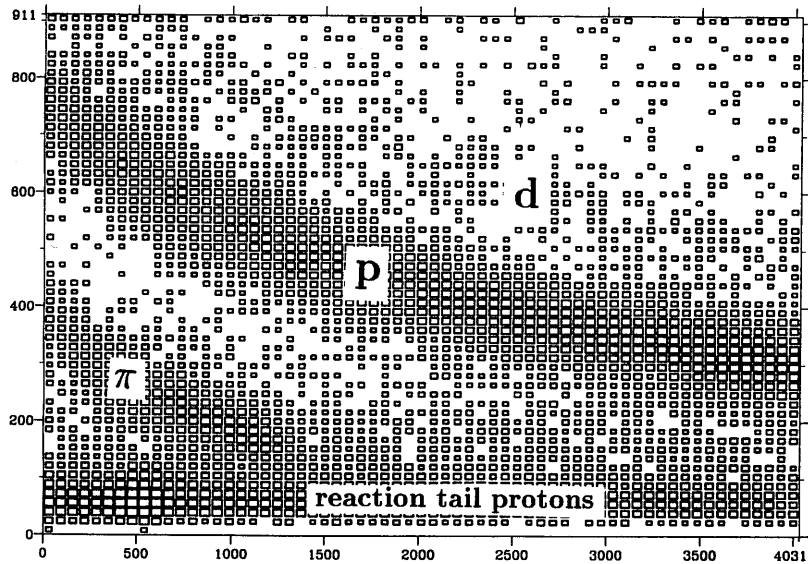


Figure 2. ΔE vs. E for particles which stopped in the E-detector. The small pion locus is clearly separated from the larger proton locus.

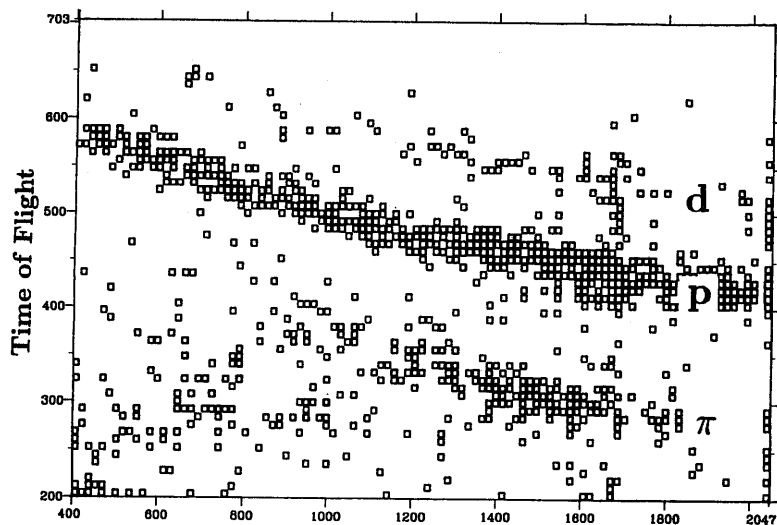


Figure 3. Time-of-flight vs. energy for particles which stopped in the ΔE detector. The time is taken between the F and ΔE detectors and is typically 5 ns for the pions of interest.

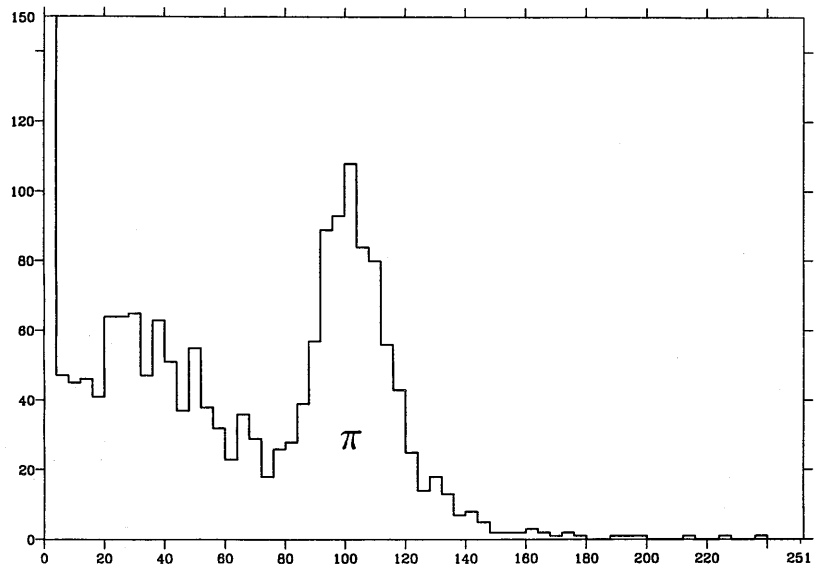


Figure 4. ADC(150-ns gate) - ADC(10-ns gate) for particles stopping in the E detector. The peak corresponds to the 4 MeV deposited by muons coming from pion decay inside the detector.

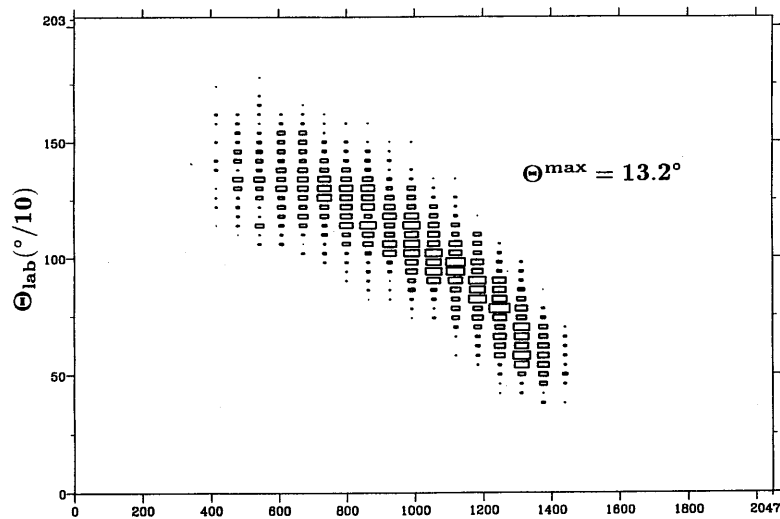


Figure 5. θ_{lab} vs. E for pions showing the half of the kinematic “parabola” corresponding to forward going pions in the CM system.